

35
VLA-MAX 91 TESTS OF HIGH ENERGY FLARE PHYSICS*Kenneth R. Lang and Robert F. Willson*

Department of Physics and Astronomy

Tufts University, Medford, MA 02155

Abstract

The potential for VLA contributions during the coming maximum in solar activity is illustrated by unpublished observations of solar flares on 28 May, 8 June, 24 June and 30 September, 1988; some of this data will appear in the two papers by Willson et al. (1989a,b) referenced at the end of this article. The VLA can be used to spatially resolve flaring active regions and their magnetic fields; these results can be compared with simultaneous X-ray and gamma ray observations from space. We provide examples in which spatially separated radio sources are resolved for the pre-burst, impulsive and decay phases of solar flares. The emergence of precursor coronal loops probably triggers the release of stored magnetic energy in adjacent coronal loops. Noise storm enhancements can originate in large-scale coronal loops on opposite sides of the visible solar disk. An interactive feedback mechanism may exist between activity in high-lying 90 cm coronal loops and lower-lying 20 cm ones.

VLA Studies of Solar Flares

The VLA can be used to spatially resolve the various components of the active solar atmosphere, thereby improving our understanding of highly energetic, eruptive phenomena such as solar flares, erupting filaments, and coronal mass ejections. This can be done by observing activity across the entire solar disk at 20 cm and 90 cm wavelength. The 20 cm observations resolve coronal loops within active regions, while the 90 cm ones detect larger-scale coronal systems such as filaments and loops that interconnect two active regions or connect one active region with remote regions on the Sun. This capability was not available during the past solar maximum.

Solar flares, or bursts, can be imaged with VLA snapshot maps over times as short as 1.67 seconds. This is possible because microwave flares have a relatively simple structure and high brightness relative to the background Sun. The potential of such observations is illustrated by unpublished 20.7 cm observations that resolve the preburst, impulsive and decay phases of a microwave burst into three spatially separated coronal loops or systems of loops. (Figures 1,2,3 and 4).

In this case, the hot, precursor source apparently interacted with an adjacent one, leading to the explosive release of energy during the impulsive phase. The system of coronal sources then seems to have relaxed to a more stable state when yet another nearby source emitted the decay phase. Such studies are related to recent X-ray satellite observations by Machado et al. (1988). They showed that X-ray flaring activity usually involves two or more interacting magnetic bipoles within an active region with an initiating bipole impacting against the adjacent one.

Another unpublished observation (Figures 5 and 6) shows 20.7 cm precursor source seen with the VLA and not detected at hard X-rays. This precursor source is unpolarized and spatially separated from the subsequent impulsive burst which is dipolar and has a time profile that is well-correlated with the hard X-ray emission.

The soft X-ray data (GOES) indicate that the precursor source cannot be due to thermal bremsstrahlung; it is interpreted as the thermal gyroresonance radiation of emerging magnetic loops that trigger subsequent impulsive bursts from nearby coronal loops. Both the temperature and dipolar structure of the impulsive radiation are explained by the gyrosynchrotron radiation of energetic electrons in a dipolar loop. The injection of these electrons also explains the simultaneous hard X-ray emission.

VLA observations will also provide insight to other explosive solar phenomena such as coronal mass ejections and/or filament eruptions that may not be associated with impulsive solar flares. Current theoretical scenarios invoke instabilities and the eruption of large-scale magnetic arcades, or helmet streamers, that drive a coronal mass ejection and initiate subsequent filament eruption and/or flare emission (Priest 1988). If these models are correct, then the initiating source and driving mechanism for coronal mass ejections may occur in the low solar corona and they might be only weakly coupled to the visible solar surface. Because the low solar corona is blocked by the occulting disks of coronagraphs, the VLA will provide one of the only ways of studying the triggering of coronal mass ejections during the coming maximum. These ejections will be subsequently viewed by coronagraphs as they propagate out through the middle and upper corona.

There is also uncertainty about the unknown source that initiates and continually excites solar noise storms for hours. Stewart, Brueckner and Dere (1986) have shown that the onset or cessation of noise storm activity is correlated with changes in large-scale coronal magnetic fields within an active region. VLA observations during MAX 91 at 20 cm and 90 cm wavelengths will provide insight to these phenomena.

Summary

The VLA can provide information on the location and method of energy release during explosive solar flares, and specify brightness and polarization structure during their

preflare, impulsive, and post-flare stages. Information on preburst heating and magnetic flare triggering can be obtained, and theoretical models for solar flares can be tested. The location of primary energy release at micro-wave wavelengths can be established. Thermal and magnetic evolution in the low solar corona can also be studied, perhaps establishing an initiating mechanism for coronal mass ejections. As discussed in another part of these workshop proceedings, in a paper entitled "VLA Capabilities for MAX 91" the VLA should be used for two-week observing campaigns in support of NASA solar observing flights. The VLA observations should also be coordinated with other ground-based telescopes to fully exploit the scientific return of the MAX 91 campaign.

References

- Machado, M.E., Moore, R.L., Hernandez, A.M., Rovira, M.G., Hagyard, M.J., and Smith, J.B. 1988, "The Observed Characteristics of Flare Energy Release. I. Magnetic Structure and the Energy Release Site." *Astrophysical Journal* 326, 425-450.
- Priest, E.R. 1989, "The Initiation of Solar Coronal Mass Ejections by Magnetic Non-Equilibrium." *Astrophysical Journal* 328, 848- 855.
- Stewart, R.T., Brueckner, G.E., and Dere, K.P. 1986, "Culgoora and Skylab EUV Observations of Emerging Magnetic Flux in the Lower Corona." *Solar Physics* 106, 107-130.
- Willson, R.F., Lang, K.R., Kerdraon, A., Klein, L., and Trottet, G. 1989, "Multi-wavelength Observations of Energy Release During a Solar Flare." Submitted to *Astronomy and Astrophysics*.
- Willson, R.F., Lang, K.R., Schmelz, J.T., and Smith, K.L. 1989, "Multiple-wavelength SMM-VLA Observations of an M2-Class X-ray Flare and an Associated Coronal Mass Ejection." Submitted to the *Astrophysical Journal*.

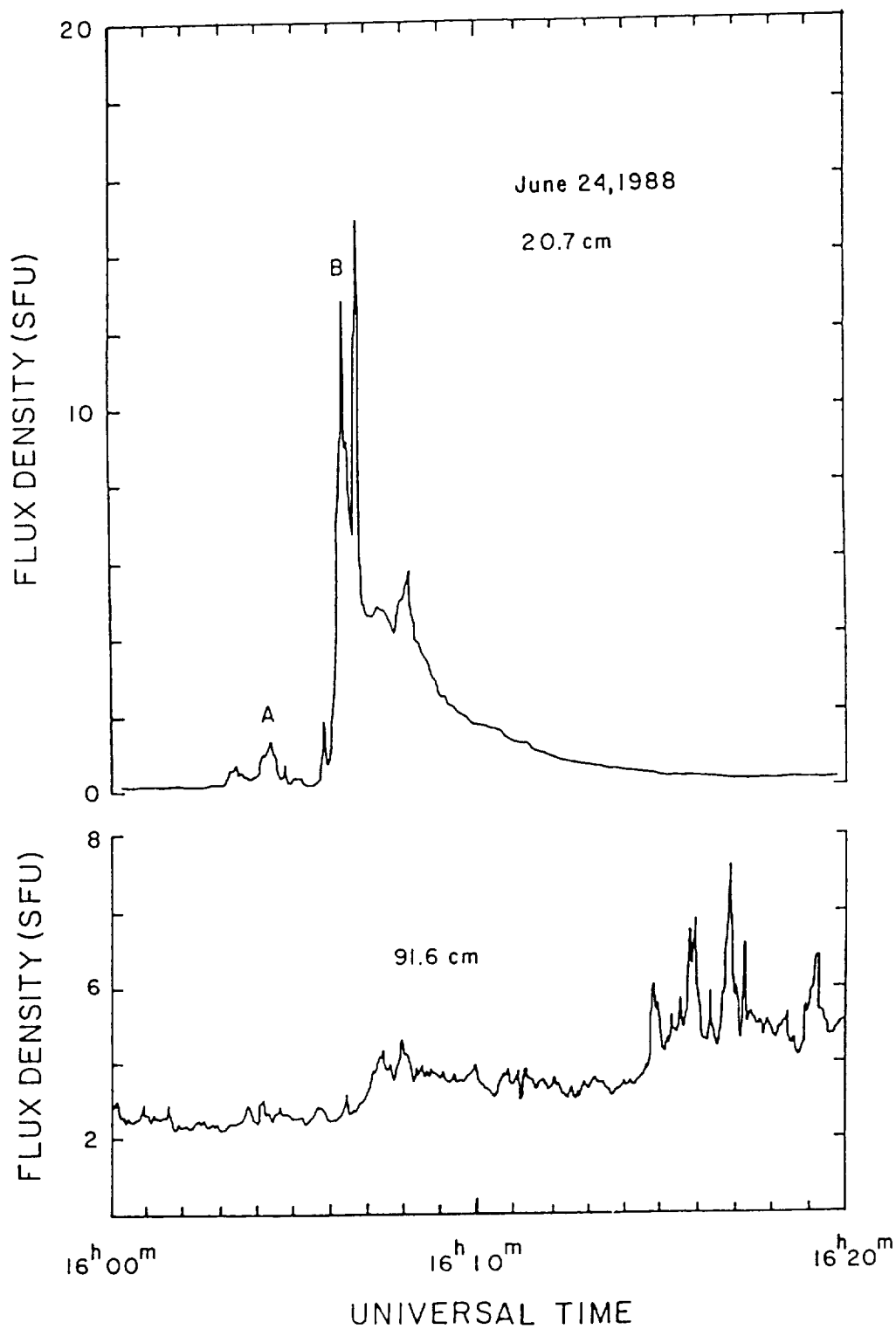


Fig. 1. The time profile of a 20.7 cm (1446 MHz) flare has a pre-burst (A), impulsive (B) and post-burst components that are spatially resolved with the VLA in different coronal sources (Figures 2 and 4). The bottom profile shows the impulsive burst and a subsequent noise storm at 91.6 cm wavelength (327.5 MHz).

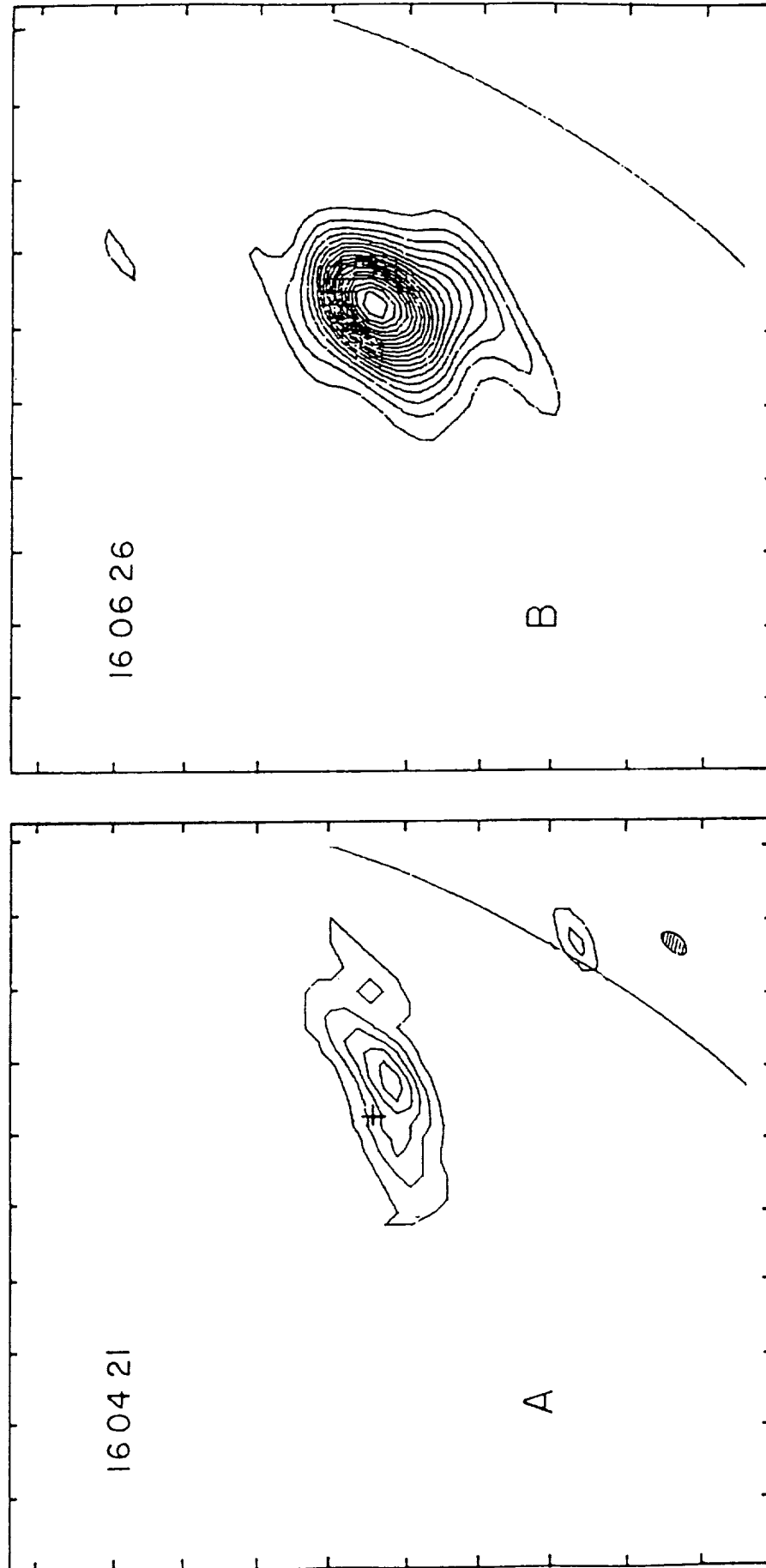


Fig. 2. The VLA resolves the preburst (A) and impulsive (B) components of a 20.7 cm flare into spatially separated components with peak brightness temperatures of $T_{B_{\max}} = 4.4 \times 10^6$ K and 1.0×10^8 K, respectively, and respective angular sizes of $\theta = 90'' \times 180''$ and $180''$.

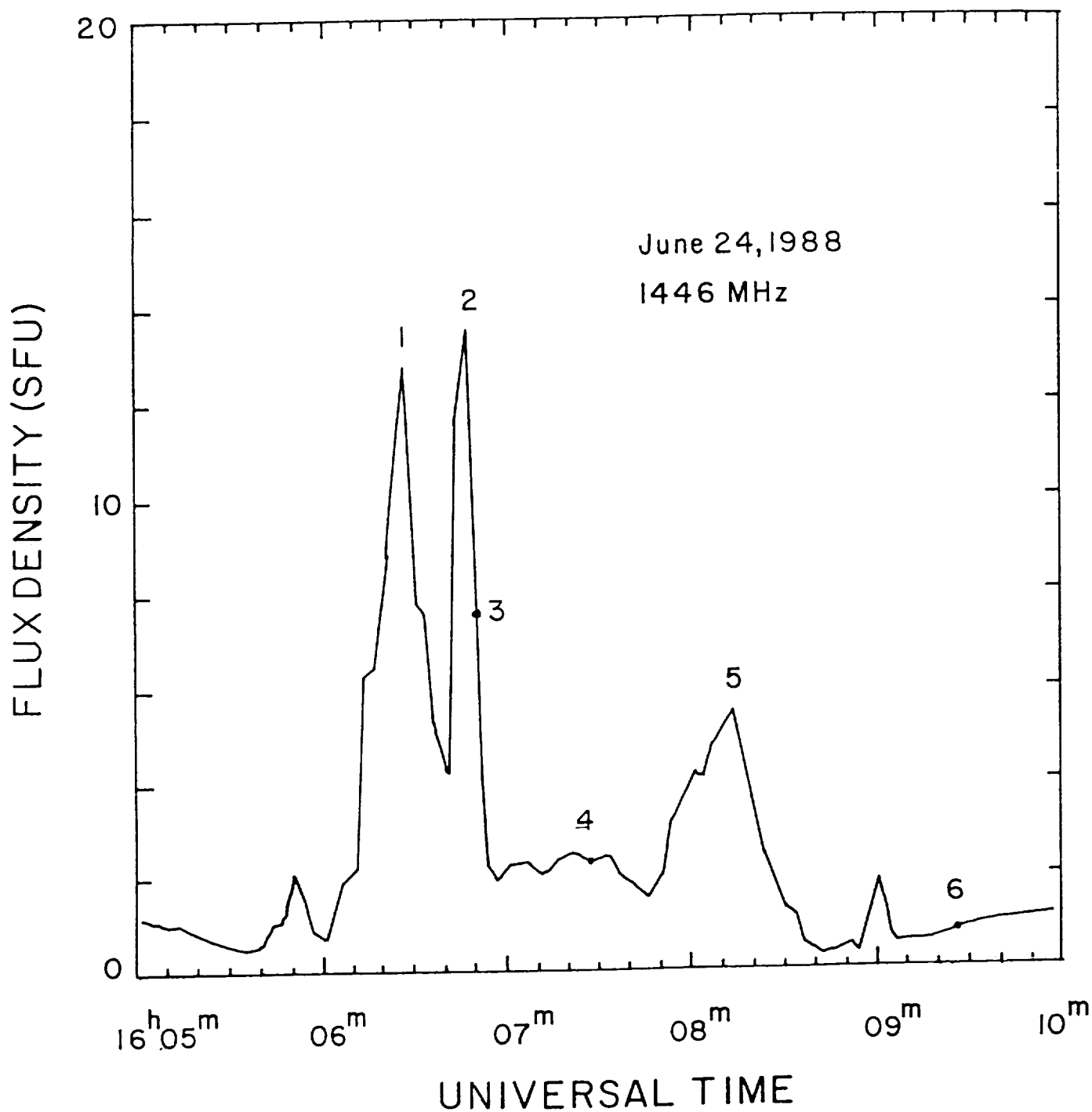


Fig. 3. An expanded time profile of the impulsive (1 and 2) and post-burst (3,4,5 and 6) components of a 20.7 cm flare. The two components come from spatially separated sources (see Figure 4).

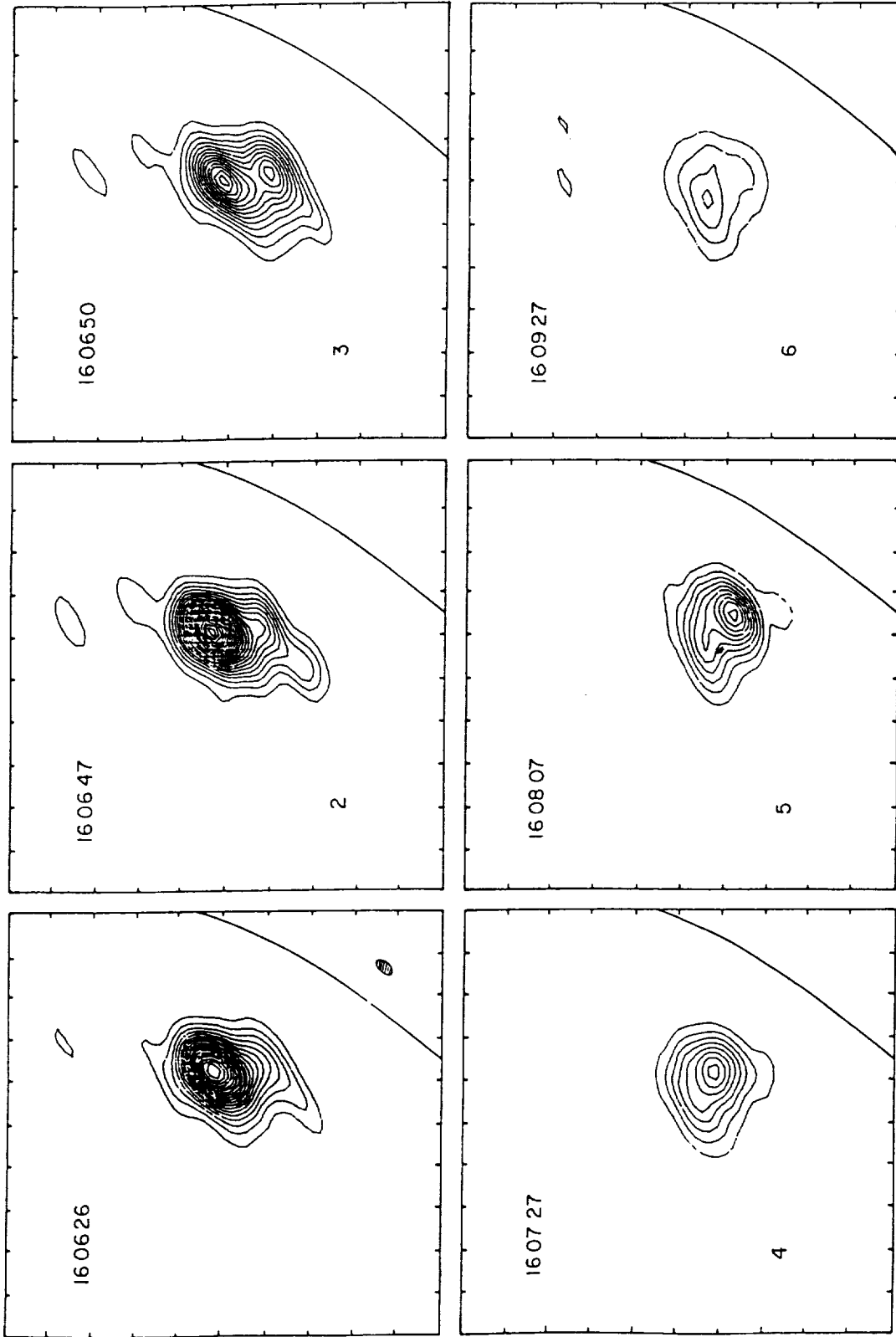


Fig. 4. The impulsive components (1 and 2) of a microwave burst are resolved with the VLA; they come from the same source with a peak brightness temperature of $T_{\text{B max}} = 1.0 \times 10^8$ K and an angular extent of $\theta = 180''$. The post-burst emission comes from a spatially separated source that was first detected during the decay of the impulsive source 2 at time 3, and remained fixed in position and size for all subsequent times 4, 5, and 6.

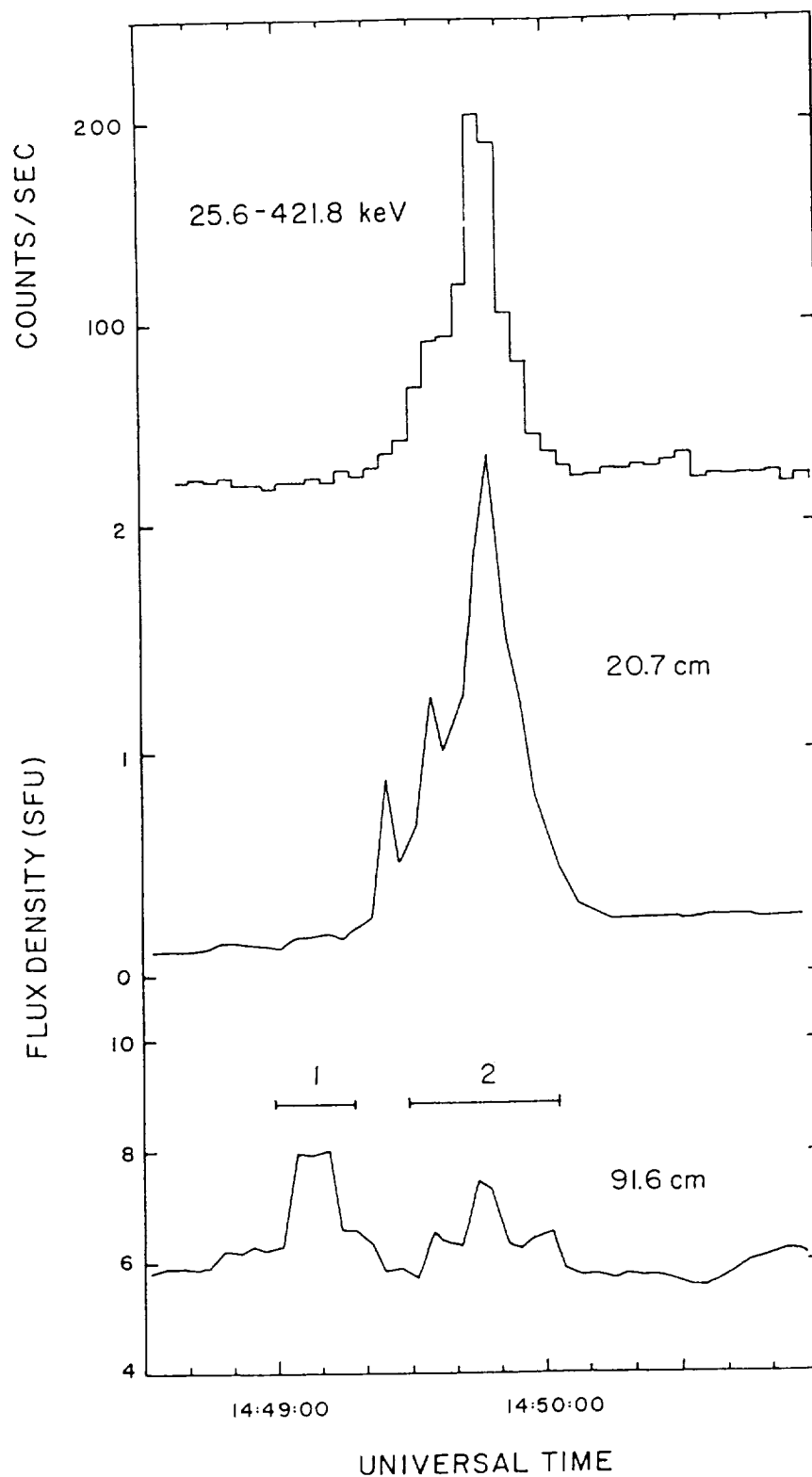


Fig. 5. The time profile of a 20.7 cm burst (middle) exhibits precursor emission that is not detected at hard X-ray wavelengths (top). Subsequent burst emission in the two spectral domains is well-correlated and is attributed to energetic electrons within a dipolar loop. The preburst and impulsive components are resolved by the VLA into two spatially separated components (see Figure 6).

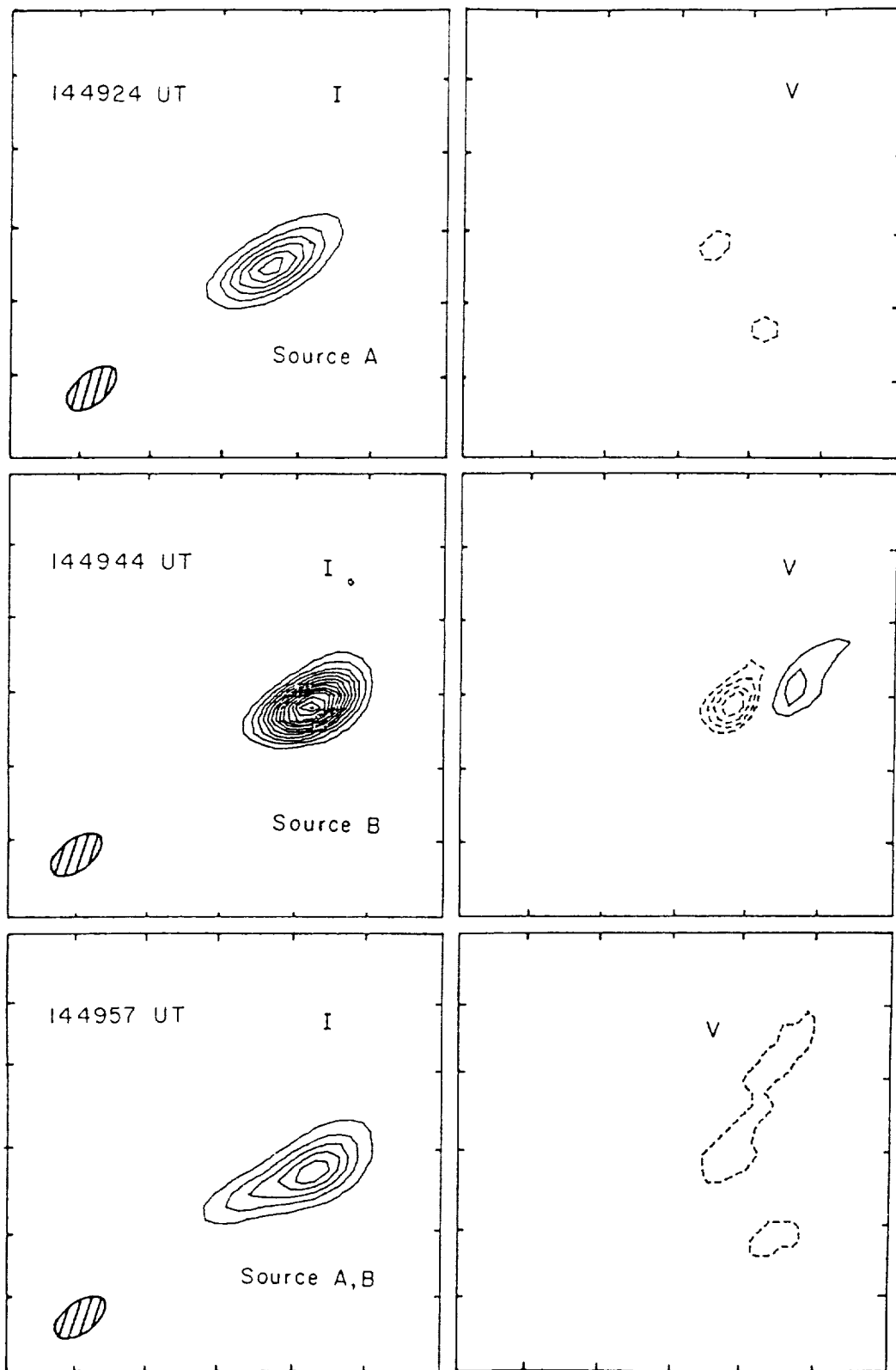


Fig. 6. The preburst emission A, is attributed to emerging coronal loops that triggered subsequent impulsive radiation from the dipolar source B. Both components have been resolved with the VLA with peak brightness temperatures of $T_{B_{\max}} = 6.6 \times 10^6$ K and 1.5×10^7 K and angular sizes of $\theta = 30'' \times 60''$.